Advanced Composite Materials
Publication details, including instructions for authors and subscription information:
http://www.tandfonline.com/loi/tacm20

Design Analysis of a 3-3 Mode Piezocomposite Actuator

Ngoc-Trung Nguyen [a] , Jin-Hwe Kweon [b] & Kwang-Joon Yoonb [c]

[a] Research Center for Aircraft Parts Technology, School of Mechanical and Aerospace Engineering, Gyeongsang National University, Jinju, Gyeongnam 660-701, South Korea, Department of Mechanical & Biomedical Engineering, Kangwon National University, Chunchon, Kangwon, 200-701, South Korea

[b] Research Center for Aircraft Parts Technology, School of Mechanical and Aerospace Engineering, Gyeongsang National University, Jinju, Gyeongnam 660-701, South Korea;, Email: jhkweon@gnu.ac.kr

[c] ASML, Artificial Muscle Research Center, Department of Aerospace Information System Engineering, Konkuk University, Seoul 143-701, South Korea

Version of record first published: 02 Apr 2012.

To cite this article: Ngoc-Trung Nguyen , Jin-Hwe Kweon & Kwang-Joon Yoonb (2011): Design Analysis of a 3-3 Mode Piezocomposite Actuator, Advanced Composite Materials, 20:4, 301-317

To link to this article: http://dx.doi.org/10.1163/092430410X550863

VSP

Advanced Composite Materials 20 (2011) 301–317

ADVANCED COMPOSITE MATERIALS
brill.nl/acm

Design Analysis of a 3–3 Mode Piezocomposite Actuator

Ngoc-Trung Nguyen [a,*], **Jin-Hwe Kweon** [a,**] **and Kwang-Joon Yoon** [b]

[a] Research Center for Aircraft Parts Technology, School of Mechanical and Aerospace Engineering, Gyeongsang National University, Jinju, Gyeongnam 660-701, South Korea

[b] ASML, Artificial Muscle Research Center, Department of Aerospace Information System Engineering, Konkuk University, Seoul 143-701, South Korea

Received 8 June 2010; accepted 19 November 2010

Abstract

In this paper, the design of a 3–3 mode unimorph piezocomposite actuator is evaluated using an analytical model. Adopting an effective lay-up structure established in earlier research by the authors, the actuator consists of an active layer operating with 3–3 mode actuation bonded to several other composite prepreg layers. The interdigitated electrodes through which the electric signal is applied to achieve 3–3 actuation along longitudinal direction are embedded into PZT ceramic. The asymptotic homogenization technique is used to calculate effective electro-mechanical properties of the active layer. These properties are then used in the analytical model to investigate the influence of the critical design parameters on the performance of the actuator through a defined coefficient. Optimal values of the active layer thickness are obtained for common electrode materials. The results demonstrate that metals having similar stiffness of the PZT ceramic are preferable as electrodes as they reduce the electrode width, bringing the design closer to an ideal case.

Keywords

d_{33}-mode, piezocomposite actuator, interdigitated electrodes, homogenization

1. Introduction

Although piezocomposite actuators show many practical advantages, the actuation they generated has remained small. An effective approach to improve the performance of a piezocomposite actuator is to apply a direct piezoelectric effect along the poling direction (employing 3–3 mode actuation) rather than to use the transverse direction (3–1 mode actuation) since the piezoelectric coefficient d_{33} is nearly twice as large as the d_{31} value [1]. The induced strain of a piezoelectric ceramic layer with a 3–3 actuation mechanism is therefore higher than that with a 3–1 mode.

* Currently working at the Department of Mechanical & Biomedical Engineering, Kangwon National University, Chunchon, Kangwon, 200-701, South Korea.

** To whom correspondence should be addressed. E-mail: jhkweon@gnu.ac.kr

Edited by the KSCM

DOI:10.1163/092430410X550863

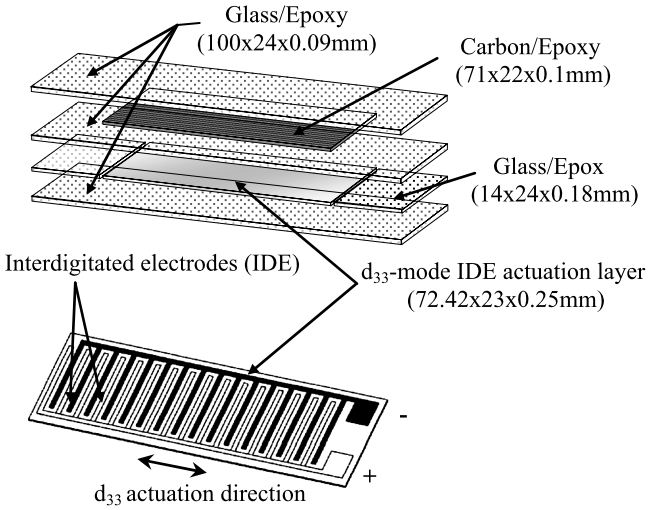

Figure 1. Layup structure of the 3–3 mode piezocomposite actuator.

AFC™ (MIT) and LaRC-MFC™ (NASA Langley Research Center) are typical examples of where 3–3 mode actuation is used to improve the actuation performance [2, 3]. With this type of actuation, interdigitated electrodes (IDEs) are patterned on the surface of piezoceramic fibers. However, the fabrication of these 3–3 mode actuators is in some ways complicated and costly. Moreover, the attenuation of the driving electric field phenomenon occurring in the AFC™/MFC™ actuators due to the unwanted accumulation of epoxy between the electrodes and ceramics remains an unsolved issue [4, 5].

Recently, Yoon *et al.* [6] proposed the concept of a stacked ceramic thin embedded InterDigitated Electrode Actuation Layer (IDEAL). The actuation layer is then co-cured with other constituent material layers in accordance with an effective lay-up design to form a unimorph piezocomposite actuator [7], as shown in Fig. 1. The piezocomposite actuator is designed to have a large actuating moment through an increase in the distance from the flexural neutral surface of the actuator to the center of the actuating layer. A glass/epoxy layer with the full length of the actuator is imbedded between the active layer and the carbon/epoxy layer to increase the moment arm distance and to prevent cracks from initiating at the edges of the ceramic wafer. Another layer of glass/epoxy is situated on the top surface of the carbon/epoxy layer to protect the active layer from external impacts and to provide electrical insulation for the carbon/epoxy top layer. The stacked layers are then vacuum bagged and cured at an elevated temperature (177°C) following an autoclave bagging process. Mismatching in the coefficient of thermal expansion of the constituent materials gives the manufactured actuators a curved shape and induces stress in each layer [8].

Improved performance of this type of actuator is attributed to the 3–3 mode actuation mechanism with the embedded IDE active layer compared to a regular

counterpart with the 3–1 mode transverse design. As the d_{33} coefficient is normally twice the d_{31} value, actuation performance of a 3–3 mode actuator is expected to be improved significantly. However, a perfect 3–3 mode actuator is not achievable because the active layer requires electrodes of finite width at which the electric signal is applied. The embedded IDE reduces the actuating efficiency by serving as non-active portions in the active layer. Moreover, the selection of the electrode material can affect the performance of the actuator by modifying the overall stiffness and piezoelectricity of the active layer. Yet no study systematically including these factors has been found in the literature so far.

This study investigates the effects of several design parameters of the active layer on the overall performance of a piezocomposite actuator. An analytical model is used to evaluate the design effectiveness through a newly defined coefficient termed the *curvature coefficient of a unimorph actuator*. Discussions on analyses in this paper suggest a guideline to design efficient 3–3 mode unimorph piezocomposite actuators.

2. The Analytical Design Model

The actuation displacement of a unimorph actuator is produced by the change in the curvature of the laminated structure when an electric field is applied on an electro active layer [8]. The actuating mechanism of a multi-layered beam structure is shown in Fig. 2.

In Fig. 2, a is the moment arm, ΔP_{a} represents the change in the actuating force of the electro active layer generated due to the change in the electric field, and ΔM_{a} represents the change in the bending moment. For an actuator beam of a unit width, the change in the curvature can be expressed as follows:

$$\Delta\kappa = \frac{1}{\Delta\rho} = \frac{\Delta M_{\mathrm{a}}}{D}. \tag{1}$$

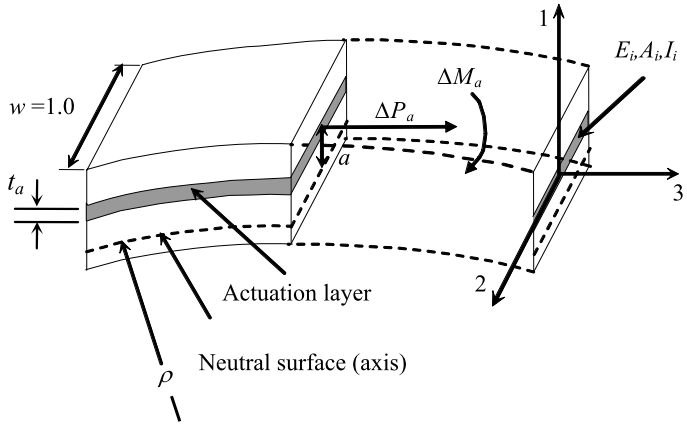

Figure 2. Curvature change of a laminated beam with electro active layer [8].

Here, $D = \sum E_i I_i$ is the total bending stiffness which is the sum of the bending stiffness of each layer with respect to the neutral axis, and E_i and I_i are the modulus (or the effective modulus) and the area moment of inertia of each layer. The change in the actuation moment ΔM_a is the vector product of the actuation force change ΔP_a and the moment arm a. The change in the actuation force ΔP_a can be obtained from the multiplication of the area of actuation layer cross-section A_a $(= 1 \times t_a)$ per unit width, the *effective* elastic modulus of the actuating layer $\overline{E}_a$, and the strain $\bar{d}_{ij} \times \Delta E$ induced from the change in the electric field where $\bar{d}_{ij}$ is the *effective* electro-active strain coefficient and ΔE is the electric field change. Therefore ΔM_a can be expressed as follows:

$$\Delta M_a = a \times t_a \times \overline{E}_a \times \bar{d}_{ij} \times \Delta E. \tag{2}$$

The change in the curvature therefore is

$$\Delta\kappa = \frac{a}{D} \times t_a \times \overline{E}_a \times \bar{d}_{ij} \times \Delta E = c_{cua} \times \Delta E, \tag{3}$$

where the *curvature coefficient of a unimorph actuator* is defined by $c_{cua} = a/Dt_a\overline{E}_a\bar{d}_{ij}$.

It is clear that the moment arm length a from the flexural neutral surface of the actuator beam to the center of the active layer must be as large as possible to have a larger actuating moment, which implies that the actuating layer should be placed on one of the outer surfaces. In addition, the total bending stiffness of an actuator section should be small to have a large curvature change for a given actuation moment. Thus, the larger is the value of c_{cua}, the higher the actuation displacement that can be achieved. This analytical model can be used to evaluate the design performance of a piezocomposite actuator and to study the contribution of each design parameter. To illustrate the usefulness of the model, the performance of two actuation modes of the actuator depicted in Fig. 1 was initially evaluated and compared. Additionally, to demonstrate the effectiveness of this model, the effect of the actuation layer thickness as a design parameter of the given actuator was investigated.

To compare the actuating performance between the d_{31}-mode and the d_{33}-mode of the actuator shown in Fig. 1, the lay-up design, materials, and dimensions were identical. The difference between two actuators is thus only the actuation mechanism of the electro active layer. Given the geometry, dimensions (in Fig. 1) and properties of the constituent materials (in Table 1) of these two piezocomposite actuators, the comparison in Table 2 was formulated. It is shown that, for the same given values of the actuating layer thickness t_a and the applied electric field change ΔE, an actuator operating with the perfect d_{33}-mode can theoretically generate a curvature change nearly twice that with the d_{31}-mode.

An appropriate selection of the ceramic wafer thickness can help reduce the operational voltage of the d_{31}-mode actuator and improve the effectiveness in the generation of the deformed shape in both cases. From equation (3), it is clear that

Table 1.
Properties of constituent materials (after [8])

Properties		PZT-5H	Carbon/epoxy	Glass/epoxy
Modulus	E_1 (GPa)	62	231.2	21.7
	E_2 (GPa)	62	7.2	21.7
	E_3 (GPa)	49	7.2	0.217
	G_{12} (i)	23.66	4.3	3.99
	ν_{12}	0.31	0.29	0.13
Piezoelectric strain coefficient	d_{31} ($\times 10^{-12}$ m/V)	−320	–	–
	d_{33} ($\times 10^{-12}$ m/V)	650	–	–
CTE	α_1 (10^{-6} K^{-1})	3.5	−1.58	14.2
	α_2 (10^{-6} K^{-1})	3.5	32.2	14.2
Product/manufacturer		3203HD, CTS	UPN-116B, SK Chemicals	GEP-108, SK Chemicals

Table 2.
Comparison of actuator performances and characteristics

Quantity	Symbol	Unit	d_{31}-mode	d_{33}-mode
Bending stiffness	D	($\times 10^{-3}$ N·m^2)	24.1	22
Moment arm	a	(mm)	0.151	0.163
Curvature coefficient	$c_{\text{cua}} = a/Dt_{\text{a}}E_{\text{a}}d_{ij}$	(V^{-1}·m^{-1})	$0.123t_{\text{a}}$	$0.236t_{\text{a}}$
Actuation moment	ΔM_{a}	($\times 10^{-3}$ N·m)	$3.0t_{\text{a}}\Delta E$	$5.2t_{\text{a}}\Delta E$
Curvature change	$\Delta\kappa = \Delta M_{\text{a}}/D$	(m^{-1})	$0.124t_{\text{a}}\Delta E$	$0.236t_{\text{a}}\Delta E$

for a piezocomposite of the given lay-up structure and the actuating layer properties, the change in curvature is higher if the value of $a/D \times t_{\text{a}}$ is larger. Here, the thickness of the active layer is included implicitly in the a/D term. The variations of $a/D \times t_{\text{a}}$ with respect to the active layer thickness for the d_{31}-mode and d_{33}-mode actuators are depicted in Fig. 3. That contribution to the curvature change of the variation of the PZT thickness can be inferred from the resulting graph. Starting from a small thickness value, the contribution increases rapidly with a thicker wafer and then reduces gradually. It is clear that with a PZT thickness of 150 μm and with the given lay-up structure, the curvature change with both d_{31}- and the d_{33}-mode actuator can result in the largest value.

As mentioned above, the fully perfect d_{33}-mode actuator is not achieved in practice due to the presence of the non-active electrode material. Instead, to fabricate a d_{33}-mode active layer, the IDE system can be patterned on the PZT surfaces or embedded into the ceramic. The former method causes *dead zones* (ineffective zones) underneath the electrode fingers in the ceramic which do not contribute to a feasible actuation mechanism, whilst the latter reduces the actuating efficiency by introduc-

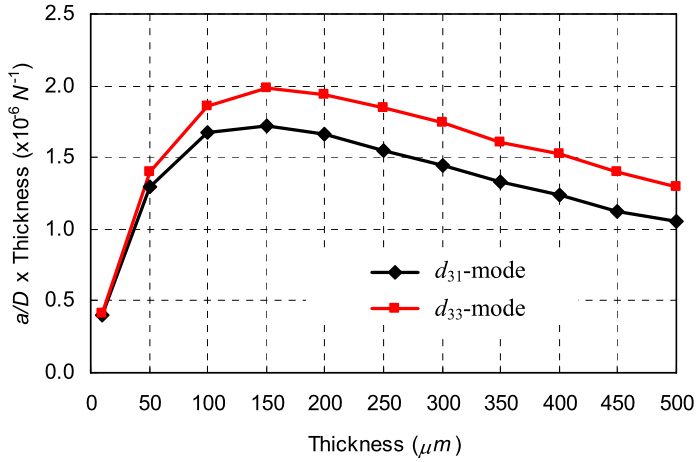

Figure 3. Variation of the term $a/D \times t_a$ with respect to the PZT thickness. This figure is published in color in the online version.

ing the embedded electrodes as non-active portions in the active layer. The next sections will discuss the effects of the volume fraction, material of the embedded electrodes and the thickness of the IDE active layer on the overall performance of the piezocomposite actuator.

3. Homogenization of the IDE Piezoceramic Active Layer

Considering an active layer, which contains an actuating material (piezoelectric ceramic) and electrodes (metal or polymer material), homogenization allows the layer to be considered as a piezoelectric material with equivalent properties known as *effective properties*. The asymptotic homogenization technique was selected for use in this study among several developed methods in the literature [9, 10]. Among various averaging techniques to estimate the effective properties of composites, the asymptotic homogenization method with periodicity conditions is preferable and was selected in this study due to its pertinent mathematical framework. Moreover, this approach directly accounts for the piezo-elastic coupling effect rather than other indirect techniques, e.g., the thermal analogy method replacing the piezoelectric effect by an equivalent thermal strain. The general homogenization method applied to piezoelectricity has no limitations regarding the volume fraction or shape of the constituents involved and is based upon the assumptions of periodicity of the microstructure and separation of the microstructure scale through an asymptotic expansion. Here, the active layer is formed through the repeated assemblage of unit cells along the 3-direction as shown in Fig. 4. Moreover, an assumption of perfect bonding between the PZT ceramic and the interdigitated electrodes applies.

There are four representations commonly employed in the theory of linear piezoelectricity to describe the coupled interaction between the electric and elastic variables. Here, the elastic strain, ε_{ij} and electric potential gradient, E_k are taken as the

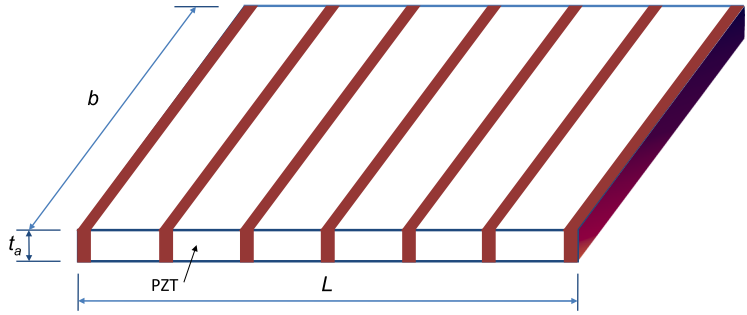

(a)

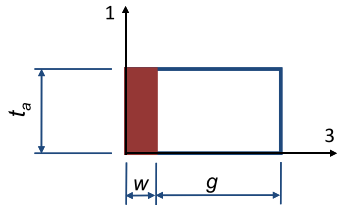

(b)

Figure 4. (a) The IDE active layer; (b) a representative volume element of the active layer containing the electrode and PZT ceramic portions. This figure is published in color in the online version.

independent variables; they are related to the stress σ_{ij} and electric displacement D_i as follows:

$$\begin{cases} \sigma_{ij} = C^E_{ijkl}\varepsilon_{kl} + e_{kij}E_k, \\ D_i = e_{ikl}\varepsilon_{kl} + \epsilon^S_{ik}E_k. \end{cases} \tag{4}$$

Here, C^E_{ijkl} is the fourth-order elasticity tensor measured in a constant electric field, ϵ^S_{ik} is the second-order dielectric tensor measured at a constant strain, and e_{kij} is the third-order piezoelectric strain tensor. Using other systems for the equations of piezoelectricity, it is possible to determine other constants, such as the S^E_{ijkl} compliance constants, the d_{ijk} piezoelectric constants, and the ϵ^T_{ik} dielectric constants. Transformation of one set of constants into another is outlined in [11].

The analytical expressions for the effective coefficients are derived by using the asymptotic homogenization method [9, 10]:

$$C^{\text{hom}}_{ijkl} = \frac{1}{|Y|}\int_Y \left(C^E_{ijkl} - C^E_{ijpq}\frac{\partial \chi^{kl}_p}{\partial y_q}\right) \mathrm{d}y,$$

$$e^{\text{hom}}_{kij} = \frac{1}{|Y|}\int_Y \left(e_{kij} - C^E_{ijpq}\frac{\partial \chi^{k}_p}{\partial y_q}\right) \mathrm{d}y,$$

where Y and $|Y|$ are the domain and the volume of a representative volume element of the active layer, respectively (Fig. 4(b)).

The functions χ_p^{kl} and χ_p^k are solutions of the so-called cell problems:

$$\frac{\partial}{\partial y_j}\left(C_{ijpq}^E \frac{\partial \chi_p^{kl}}{\partial y_q}\right) = -\frac{\partial C_{ijkl}^E}{\partial y_j}, \qquad \frac{\partial}{\partial y_j}\left(C_{ijpq}^E \frac{\partial \chi_p^{k}}{\partial y_q}\right) = \frac{\partial e_{kij}}{\partial y_j}.$$

For the specific case of the transversely layered piezoelectric composite of the active layer in this study, the effective elasticity and piezoelectricity constants are

$$C_{ijkl}^{\text{hom}} = \langle C_{ijkl}^E \rangle - \langle C_{ijm3}^E (C_{m3q3}^E)^{-1} C_{q3kl}^E \rangle + \langle C_{ijm3}^E (C_{m3q3}^E)^{-1} \rangle \langle (C_{q3p3}^E)^{-1} \rangle^{-1} \langle (C_{p3n3}^E)^{-1} C_{n3kl}^E \rangle,$$

$$e_{kij}^{\text{hom}} = \langle e_{kij} \rangle - \langle C_{ijm3}^E (C_{m3n3}^E)^{-1} e_{n3k} \rangle + \langle C_{ijm3}^E (C_{m3n3}^E)^{-1} \rangle \langle (C_{n3s3}^E)^{-1} \rangle^{-1} \langle (C_{s3q3}^E)^{-1} e_{q3k} \rangle,$$

where the quantities in the angled brackets represent the average quantities obtained by $\langle \cdot \rangle = 1/|Y| \int_Y (\cdot)\, \mathrm{d}y$.

In the next section the effect of different factors on the effective properties of the active layer are investigated. These factors are the stiffness of the electrodes, the volume fraction v_{IDE} of the electrode material, and the thickness of the PZT ceramic.

4. Results and Discussion

Considering the advantages of the lay-up structure from previous studies [7, 8], the principal design variables for the piezocomposite actuator in this study are the electrode width (w), the gap between the electrodes (g) and the thickness of the PZT ceramic layer as shown in Fig. 4. The range of values for each variable is constrained by the fabrication capabilities and the operating conditions. Depending on the manufacturing technique, the width of the IDE fingers and the gaps (g) between them cannot be smaller than the resolution limitation of that process (e.g., chemical etching, laser cutting, and/or dicing), for instance 10 μm. In fact, with a large gap, the operating voltage will increase to achieve the same electric field value. This may be a problem with autonomous applications which require a lightweight on-board power supply. The gap is thus constrained to a maximum value according to the working range of the on-board power supplier.

A non-independent variable, the volume fraction of electrode material v_{IDE}, is introduced to link the width and the distance between IDE fingers. The new variable sufficiently describes the influence on the design performance of the two variables it links. When the width of the IDE fingers is kept constant, v_{IDE} can be varied by changing the distance between the IDE fingers. On the other hand, when the gap between IDE fingers is fixed, a change in the width of the IDE fingers also

Table 3.
Mechanical properties of different electrode materials

Properties		Platinum	Gold	Silver	Copper	Aluminum	Conductive epoxy
Young's modulus	E (GPa)	168	77	83	110	70	2.5
Poisson's ratio	υ	0.38	0.44	0.37	0.34	0.35	0.4

leads to variation of the v_{IDE} value. The results in this section show the influence of the change in the volume fraction of the electrode material on the effective electro-mechanical properties of the active layer. In addition, the value of the gap ($g = 250$ μm) will also be referred for comparison purposes with a regular 3–1 mode actuator. The effects of the PZT ceramic thickness (equal to thickness of the active layer) on the overall performance for several electrode materials are then studied. Together with two typical sets of electrode gaps and width values (not the correlation between them, the volume fraction v_{IDE}), a comparison of the intermediate term in equation (3) is made to give a better sense of the sensitivity of change in the thickness. By observation, the optimal value of the thickness of the active layer can be obtained. Finally, comparisons of the curvature coefficient c_{cua} for different 3–3 mode IDE actuator designs with various electrode materials are made to quantify the amount of improvement to the 3–1 mode and how far it is from an ideal 3–3 mode actuator.

In what follows, we investigate a variety of electrode materials, including a number of common metals (gold, platinum, silver, copper and aluminum) along with a polymer (conductive epoxy). The mechanical properties of electrode materials are given in Table 3. The electro-mechanical properties of the PZT-5H ceramic were obtained from the CTS Corporation website (www.ctscorp.com). Some missing data can be inferred from equivalent ceramic types of other manufacturers (e.g., http://www.trstechnologies.com or [12]).

4.1. Effective Electro-Mechanical Properties of the Embedded IDE Active Layer

Following the homogenization approach discussed in the previous section, effective electromechanical properties of the IDE active layer are determined. Figure 5 shows the variation of the effective Young's modulus along the poled direction (the 3 axis) with respect to the volume fraction of different electrode materials. It is clear that the effective mechanical property of the active layer strongly depends on the difference in the stiffness of the electrode materials and the PZT ceramics. If the electrode material is stiffer than the ceramics, the effective value is increased, whereas it decreases if the electrode is softer. With a moderate difference, as in the case of gold, silver aluminum and copper electrodes, the effective stiffness of the active layer increases linearly with a higher volume fraction of the electrode material. Although the costs are much different, these three materials have a similar

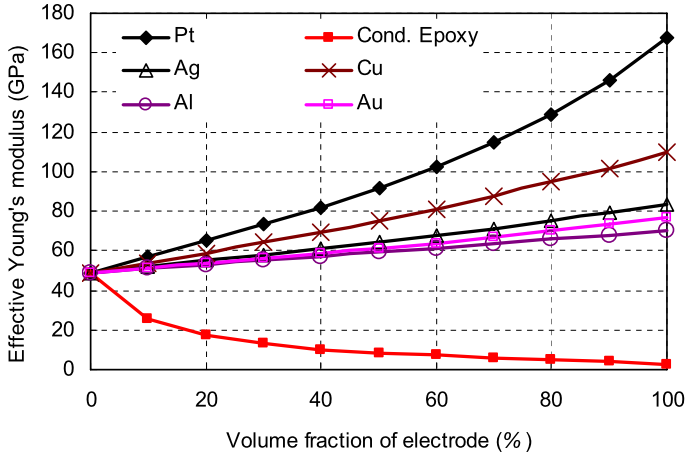

Figure 5. Effects of the material selection and volume fraction of the embedded electrode on the effective mechanical property of the active layer. This figure is published in color in the online version.

contribution to the effective property. The variations are no longer linear for platinum, copper and epoxy electrodes, whose differences are significant. The results obtained in this particular case are similar to that of Reuss's model [13].

The effective piezoelectric coefficients along the poled direction of the active layer were also investigated with different materials and while varying the volume fraction of the electrodes. Two extreme cases are considered to verify the analysis. The electromechanical properties of the active layer are those of the PZT ceramic for $v_{\mathrm{IDE}} = 0$ and are equal to the electrode values for $v_{\mathrm{IDE}} = 100\%$. In the latter case, the active layer has no piezoelectricity. Between these two extreme values, the electromechanical properties of the active layer are strongly dependent on the volume fraction of electrode material. Figure 6 shows that with a stiffer electrode, a reduction in the piezoelectricity of the active layer is higher as the volume fraction of the electrode increases. Once again, it is clear that gold, silver and aluminum electrodes make nearly the same contribution to the effective piezoelectricity of the active layer.

By combining the two graphs above, the term $\overline{E}_{\mathrm{a}} \times \bar{d}_{ij}$ in equation (3) is plotted with respect to volume fraction of the electrode in Fig. 7. This product decreases nearly linearly as the volume fraction increases for metal electrodes; however, it is strongly nonlinear for a polymer electrode. Moreover, these values with different metal electrodes are nearly identical when $v_{\mathrm{IDE}} = 0$–25%. As a consequence of the reduction in $\overline{E}_{\mathrm{a}} \times \bar{d}_{ij}$, the curvature change tends to decrease as the electrodes become thicker or as the distances between them become narrower.

According to the graphs above, an aluminum electrode can contribute equivalently to the effective properties compared to gold and silver electrodes. An aluminum electrode is selected as a representative of this group. Thus, the following discussion only investigates the cases of platinum, copper, aluminum and conduc-

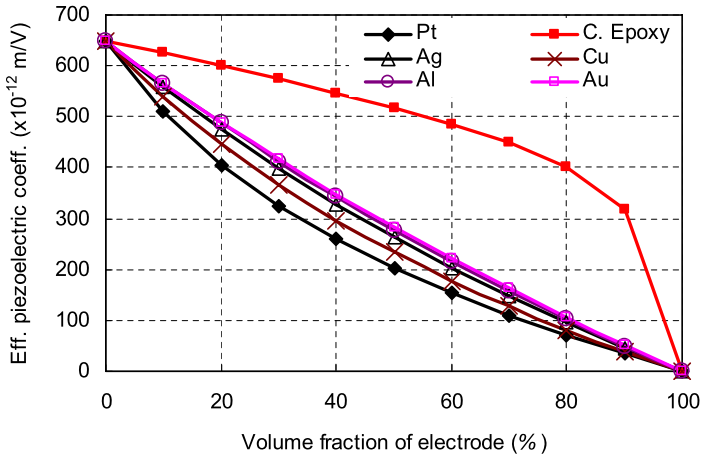

Figure 6. Effects of the material selection and volume fraction of the embedded electrode on the effective piezoelectric property of the active layer. This figure is published in color in the online version.

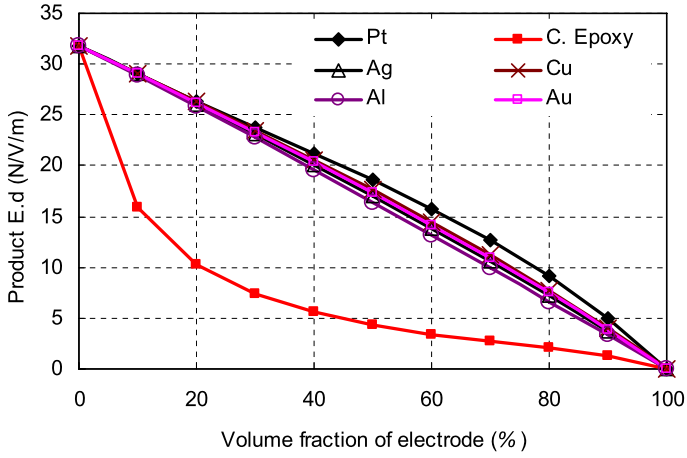

Figure 7. Variation of the term $\overline{E}_a \times \bar{d}_{ij}$ when the volume fraction of the electrode changes. This figure is published in color in the online version.

tive epoxy electrodes. Moreover, to achieve a better sense of the improvement of a 3–3 mode actuator relative to its 3–1 mode counterpart, the choice in the following consideration uses the same reference for comparison. In this case, an identical operating voltage applied to both cases generates the same electric field in the PZT ceramics. Explicitly, this condition implies that the gap between the two electrodes should be 250 μm in both cases. Distinct actuating mechanisms generate dissimilar strain outputs and thus lead to different performances. The results will show how effective a design can be by evaluating how close it is to an ideal actuator.

4.2. Effects of the Active Layer Thickness

Similar to what has been done with the 3–1 mode and the ideal 3–3 mode actuators in Section 2, the effects of the PZT ceramic thickness on the curvature change for several electrode materials of a 3–3 mode IDE actuator are investigated in this discussion. Plots of the term $a/D \times t_a$ in equation (3) for several designs show the contribution of the active layer thickness to the curvature change of those designs. In case of metal electrodes, by keeping the distance between the electrodes constant ($g = 250$ μm), the values of $a/D \times t_a$ decrease when the electrodes become thicker. In other words, the product becomes smaller if the volume fraction of the electrode material is higher. Consequently, the curvature change is reduced as the width of the electrode is increased. Hence, a good design should have electrodes that are as thin as possible. Figure 8 shows a limited case of a design in which $w = 10$ μm ($v_{IDE} = 3.8\%$) represents the finest resolution of an electrode width that can be achieved by current fabrication methods. Figure 9 shows another limited case in this analysis in which the width of the electrodes has a maximum value $w = 150$ μm ($v_{IDE} = 37.5\%$). The graphs in Figs 8 and 9 further support the finding that the product $a/D \times t_a$ decreases when the electrode width value changes from $w =$ 10 μm to $w = 150$ μm. The optimal thickness value for an active layer with a given electrode material can easily be obtained from Figs 8 and 9. These values for various metal electrodes remain unchanged for all designs. This value was determined to be 150 μm. However, for a conductive epoxy electrode, the optimal values are different in the two cases. When $w = 10$ μm, a thickness of 200 μm is the optimal value, whereas a thickness of approximately 300 μm is the optimal value for the $w =$ 150 μm design.

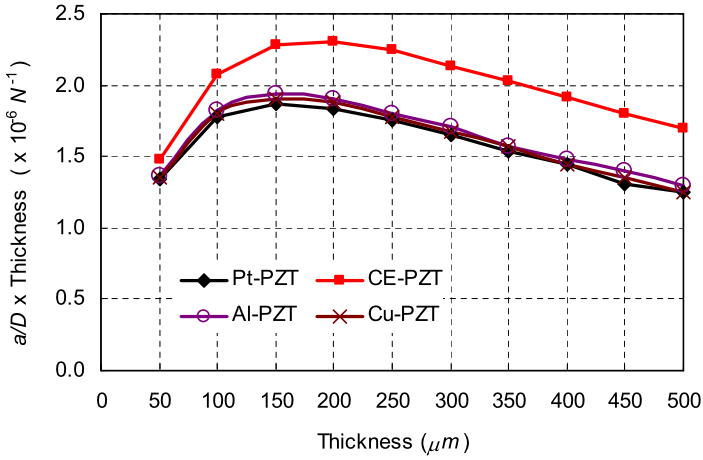

Figure 8. Variation of the term $a/D \times t_a$ according to a change in the thickness of the active layer. Case $g = 250$ μm, $w = 10$ μm ($v_{IDE} = 3.8\%$). This figure is published in color in the online version.

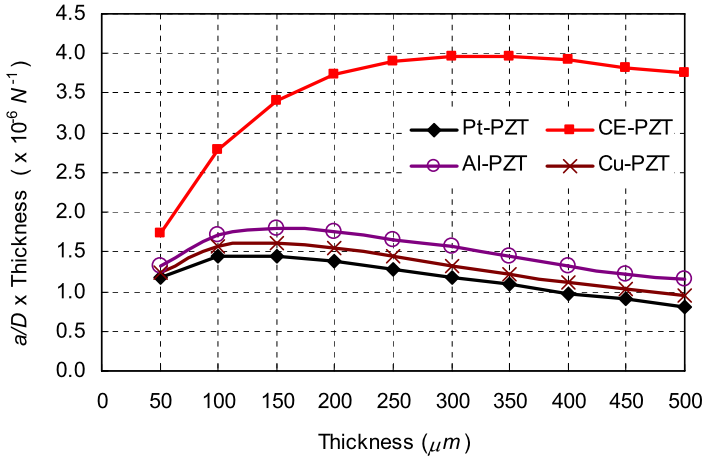

Figure 9. Variation of the term $a/D \times t_a$ according to a change in the thickness of the active layer. Case $g = 250$ μm, $w = 150$ μm ($v_{IDE} = 37.5\%$). This figure is published in color in the online version.

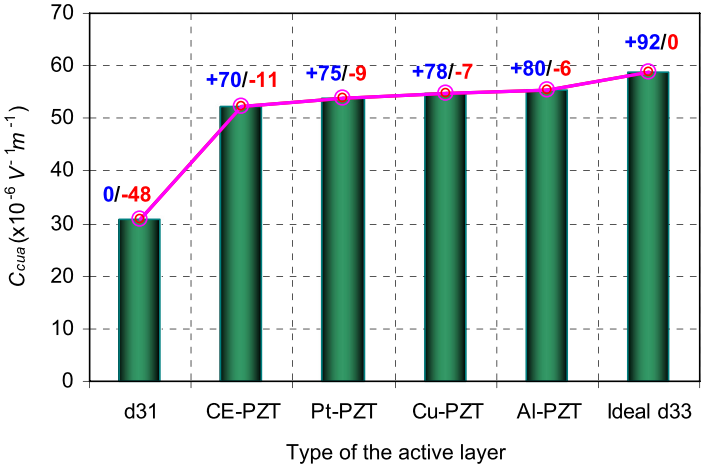

Figure 10. Comparison of the curvature coefficient of a unimorph actuator values for several electrode materials. Case $g = 250$ μm, $w = 10$ μm ($v_{IDE} = 3.8\%$). This figure is published in color in the online version.

4.3. *Evaluation of the Curvature Coefficient of a Unimorph Actuator*

As presented in Section 2, the curvature coefficient $c_{cua} = a/Dt_a\overline{E}_a\bar{d}_{ij}$ is used to evaluate the performance of a piezocomposite actuator design. A comparison of the c_{cua} values among different designs with various electrode materials leads to a better understanding of the contribution of the design parameters, not only qualitatively but also quantitatively. Figures 10–13 quantify the improvement of a 3–3 mode IDE actuator compared with its 3–1 mode counterpart and display how close it is to an ideal design. Above each column, the two numbers separated by a slash

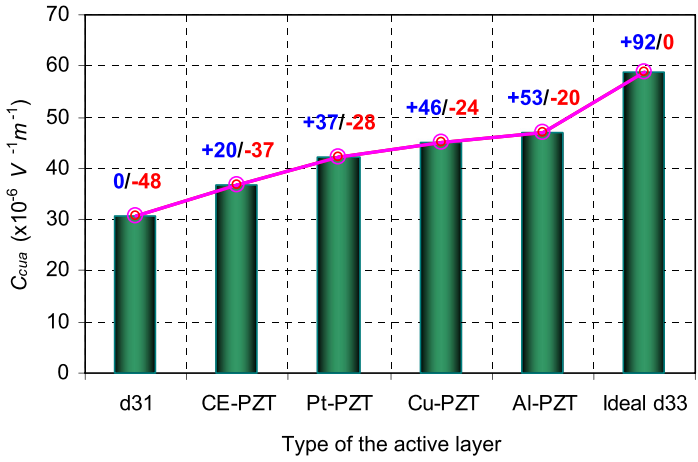

Figure 11. Comparison of the curvature coefficient of a unimorph actuator values for several electrode materials. Case $g = 250$ μm, $w = 50$ μm ($v_{\mathrm{IDE}} = 16.7\%$). This figure is published in color in the online version.

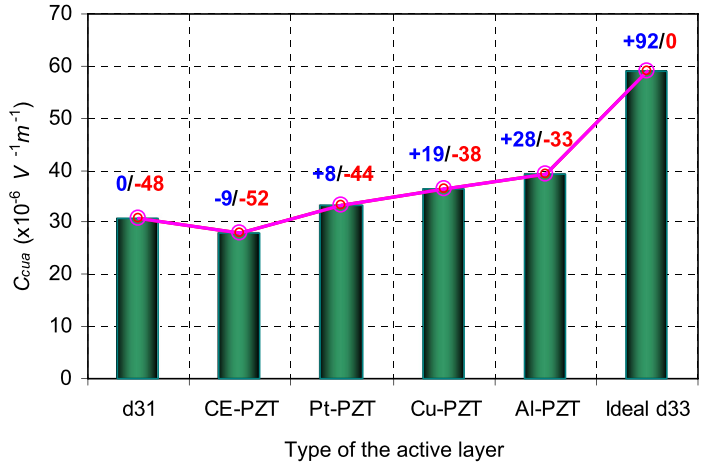

Figure 12. Comparison of the curvature coefficient of a unimorph actuator values for several electrode materials. Case $g = 250$ μm, $w = 100$ μm ($v_{\mathrm{IDE}} = 28.6\%$). This figure is published in color in the online version.

sign indicate the amount of improvement to a regular actuator and the deviation from a perfect actuator, respectively. The left number (in blue color) shows the former comparison and the right number (in red color) depicts the latter in percent. The plus (+) and minus (−) signs imply an increase and a decrease, respectively. Figure 10 shows designs with $g = 250$ μm, $w = 10$ μm and $t_{\mathrm{a}} = 250$ μm with all electrode materials. They all show a significant improvement over the regular 3–1 mode actuator (increases of 70, 75, 78 and 80% for conductive epoxy, platinum, copper and aluminum, respectively) and approach an ideal 3–3 mode mechanism

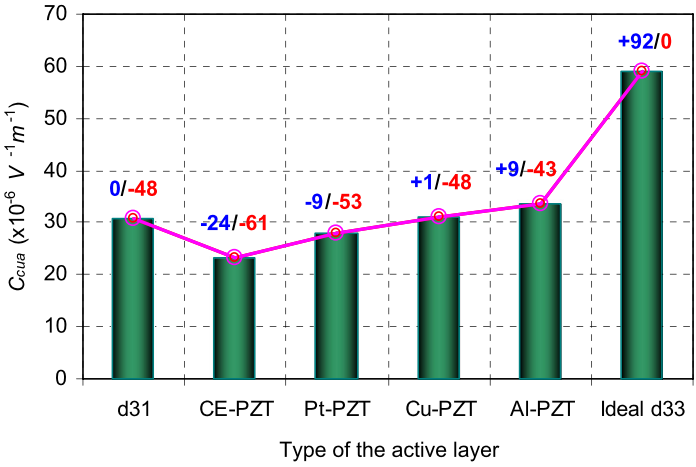

Figure 13. Comparison of the curvature coefficient of a unimorph actuator values for several electrode materials. Case $g = 250$ μm, $w = 150$ μm ($v_{\mathrm{IDE}} = 37.5\%$). This figure is published in color in the online version.

(the discrepancies are 11, 9, 7 and 6% for conductive epoxy, platinum, copper and aluminum, respectively). Similarly, other comparisons are given in Figs 11, 12 and 13 for various values of the electrode width. In this case, comparisons are carried out with the same active layer thickness, $t_{\mathrm{a}} = 250$ μm, for all designs.

In all cases, the actuator with the aluminum electrode results in the best performance through an evaluation of the curvature coefficient, c_{cua}. On the other side, the conductive epoxy electrode has the smallest value of c_{cua} among all considered analyses. The tendency of the reduction in c_{cua} as the electrode width becomes thicker is again confirmed. Moreover, the stiffness of the electrode materials is the major factor in the reduction of the effective piezoelectricity and thus reduces the actuating capability of the active layer.

5. Conclusion

This paper introduces a systematic method to evaluate the effectiveness of a 3–3 mode unimorph piezocomposite actuator through an analytical model. The performance of the design can be characterized by an efficient coefficient defined in this work which takes into account the overall layup structure of the actuator and the actuating capability of the active layer. In addition, a parametric study was conducted to investigate the effects of critical design variables on the performance of the device. In conjunction with the mathematical homogenization method, the analytical model can effectively quantify the influence of the active layer architecture associated with the geometry, distribution and choice of embedded interdigitated electrodes.

Improved performance of the actuator in question over a regular counterpart is attributed to the 3–3 mode actuation mechanism. Investigating the effects of the

design parameters, including the thickness of the active layer, the choice of the electrode material, and the correlation of the width and distance between the electrodes lend insight into the design of actuators. Comparisons with a regular 3–1 mode and an ideal 3–3 mode counterpart measured the effectiveness of the 3–3 mode embedded IDE actuator design with a given design variable set. The reduction in the actuating capability due to the embedded inactive electrode material should be minimized by narrowing the electrode fingers. Moreover, the results show that electrode materials having a stiffness value closer to the PZT ceramic value may make a better contribution to the actuator performance. As the stiffness value of aluminum is comparable to that of a piezoceramic and with a similar low cost, this material is a suitable choice as an electrode. Nevertheless, there are little differences in performance between Pt, Cu and Al when the electrode width is narrow down to 10 μm, while the differences grow as the width increases. Therefore, manufacturability and the interfacial strength issue might be more critical in electrode materials selection. The results of this study can be used as a guideline for the design work of the embedded IDE active layer in 3–3 mode unimorph piezocomposite actuators and similar types of actuators.

Acknowledgements

This work was supported by the Priority Research Centers Program through the National Research Foundation of Korea (NRF) funded by the Ministry of Education, Science and Technology (2009-0094015). Financial support from the Aerospace Parts Technology Development Project funded by the Ministry of Knowledge Economy of Korea is also acknowledged.

References

1. N. T. Nguyen, B. S. Yoon and K. J. Yoon, An improved design of piezo-composite actuator used as the artificial muscle for bio-inspired robots, in: *IEEE Intl Conf. Robotics and Biomimetics*, pp. 7–12, Sanya, China (2007).
2. A. A. Bent and N. W. Hagood, Piezoelectric fiber composites with interdigitated electrodes, *J. Intelligent Mater. Syst. Struct.* **8**, 903–919 (1997).
3. W. K. Wilkie, R. G. Bryant, J. W. High, R. L. Fox, R. F. Hellbaum, J. A. Jalink, B. D. Little and P. H. Mirick, Low-cost piezocomposite actuator for structural control applications, in: *SPIE 7th Ann. Intl Sympos. Smart Struct. Mater.*, pp. 323–334, Newport Beach, CA, USA (2000).
4. W. Wilkie, W. Williams, J. High and D. Inman, Recent Developments in NASA piezocomposite actuator technology, in: *Actuator 2004: 9th Intl Conf. New Actuators*, Paper A 4.9, Bremen, Germany (2004).
5. R. G. Bryant, *Overview of NASA Langley's Piezoelectric Ceramic Packaging Technology and Applications*, NASA Technical Report, NASA Langley Research Center, USA (2007).
6. K. J. Yoon, Y. S. Yoon, H. C. Park and N. S. Goo, *Electro Active Material Actuator Embedded with Interdigitated Electrodes*, Intl Appl. No. PCT/KR2005/003417 (2005).

7. K. J. Yoon, S. Shin, H. C. Park and N. S. Goo, Design and manufacture of a lightweight piezo-composite curved actuator, *Smart Mater. Struct.* **11**, 163–168 (2002).
8. K. J. Yoon, K. H. Park, S. K. Lee, N. S. Goo and H. C. Park, Analytical design model for a piezo-composite unimorph actuator and its verification using lightweight piezo-composite curved actuators, *Smart Mater. Struct.* **13**, 459–467 (2004).
9. A. Bensoussan, J.-L. Lions and G. Papanicolaou, *Asymptotic Analysis for Periodic Structures*. North-Holland Publishing Company, The Netherlands (1978).
10. E. Sanchez-Palencia and A. Zaoui (Eds), *Homogenization Techniques for Composite Media*. Springer, Berlin (1987).
11. *ANSI/IEEE, IEEE Standard on Piezoelectricity*, IEEE Standard, pp. 176–1987 (1987).
12. D. Berlincourt, H. H. A. Krueger and C. Near, *Properties of Morgan Electro Ceramic Ceramics*, Technical Publication TP-226, Morgan Electro Ceramics (2003).
13. R. M. Jones, *Mechanics of Composite Materials*. McGraw-Hill, New York (1975).